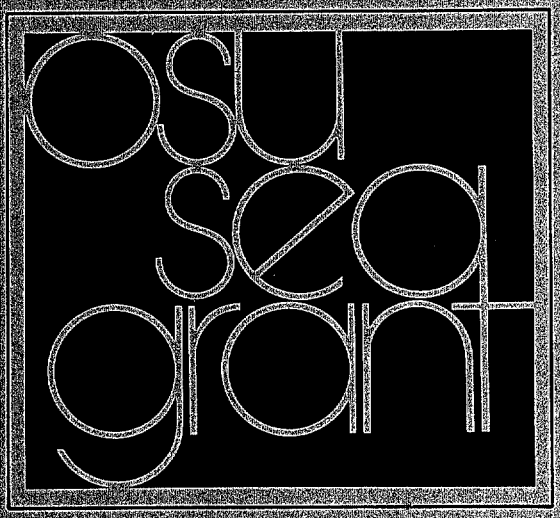

EVALUATION OF SAND WAVES IN AN ESTUARY

B. R. Baliga and Robert T. Hudspeth, M. ASCE

Reprinted from **Journal of the Hydraulics Division**, ASCE, Vol. 107, No. HY2, Proc. Paper 16016, February, 1981, pp. 161-178.

OREGON STATE UNIVERSITY
SEA GRANT COLLEGE PROGRAM
Publication no. ORESU-R-81-003

JOURNAL OF THE HYDRAULICS DIVISION

EVALUATION OF SAND WAVES IN AN ESTUARY

By B. R. Baliga[1] and Robert T. Hudspeth,[2] M. ASCE

INTRODUCTION

The National Environmental Policy Act (NEPA) establishes continuing environmental responsibilities for agencies of the Federal government [20, Sec 101(b)]. One of these responsibilities is the preparation of environmental impact statements (EIS) for dredging operations which require Federal action [20, Sec 102(2)(C)]. A comprehensive interdisciplinary methodology for identifying the chronic environmental impacts of dredging operations in estuaries has been developed by Bella and Williamson (2). A methodology for incorporating an evaluation of these environmental impacts into an environmental strategy has been outlined by Bella and Overton (1). The power of this diagnostic approach toward the preparation and evaluation of EIS for estuarine dredging lies in its relatively simple methodology for integrating disciplinary data which are easily measured, into a two-dimensional dissection plane from which the chronic impacts of dredging operations may be identified. The Bella-Williamson dissection plane approach should result in significant economic savings due to the elimination of the collection and analyses of irrelevant environmental data from estuaries in which dredging operations are proposed. Included in the Bella-Williamson dissection plane methodology are estuaries in which sand waves are present at the benthic interface; and the collection and analyses of sand wave data by spectral methods are presented in the context of a disciplinary element in the holistic dissection plane approach for diagnosing the environmental impacts of dredging in estuaries.

The two orthogonal dimensions identified by Bella and Williamson (2) for their dissection plane are: (1) The *rate of sediment turnover* (RST abscissa);

[1]Grad. Research Asst., Dept. of Civ. Engrg. and Ocean Engrg. Programs, Oregon State Univ., Corvallis, Oreg. 97331.

[2]Assoc. Prof., Dept. of Civ. Engrg. and Ocean Engrg. Programs, Oregon State Univ., Corvallis, Oreg. 97331.

Note.—Discussion open until July 1, 1981. To extend the closing date one month, a written request must be filed with the Manager of Technical and Professional Publications, ASCE. Manuscript was submitted for review for possible publication on January 24, 1980. This paper is part of the Journal of the Hydraulics Division, Proceedings of the American Society of Civil Engineers, ©ASCE, Vol. 107, No. HY2, February, 1981. ISSN 0044-769X/81/0002-0161/$01.00.

and (2) the *organic content of the sediment* (OCS ordinate). Contours of measures of the various physical, chemical, and biological environmental properties of an estuarine ecosystem may be displayed on this dissection plane with the RST and the OCS as the axes. From these contours on this dissection plane, the environmental impacts from dredging on the estuarine ecosystem may be estimated from known or predicted alterations in the RST and the OCS. Changes in the RST may be diagnosed from the direct influence of the hydrodynamic forces on sand waves at the benthic interface of an estuary. Accordingly, sand waves subjected to hydrodynamic forces due to oscillatory flows in an estuary were observed in order to estimate the RST in a *pristine* estuary. These observations from a *pristine* estuary are also compared with sand waves in an adjacent *developed* estuary.

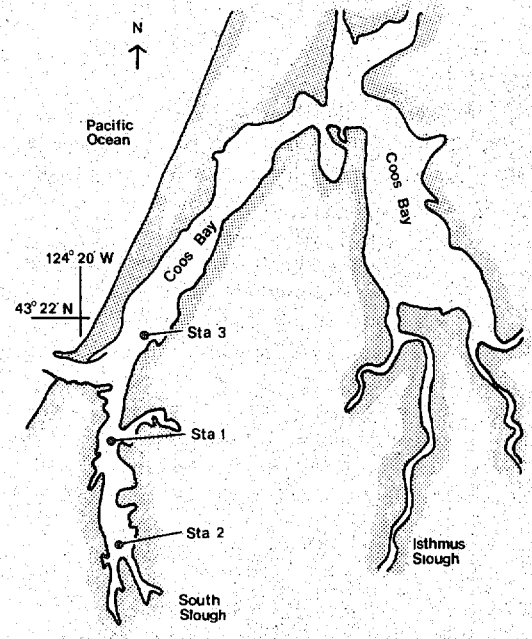

FIG. 1.—Location of Sand Wave Sampling Stations, Coos Bay Estuary, Oregon

The hydrodynamic forces which directly influence the RST at an erodible sediment interface result in an alternating sequence of erosion and deposition. In those instances when this alternating sequence of erosion and deposition result in a wave-like deformation of the sediment boundary, wave propagation theories may be employed to compute the wave celerity, C, wave length, L, and wave period, T, of these waves. In deterministic wave propagation problems, the reciprocal of the interval of periodicity yields the frequency, f, at which the process is periodically repeated and provides an estimate of the RST. Since the benthic interfaces in most estuaries are definitely not purely sinusoidal or strictly periodic, the superposition of many waves may be employed to Fourier analyze the instantaneous profile of this random interface. In addition, the

hydraulic processes which result in erosion and deposition are not, in general, deterministic and the methods of Fourier analyses may be further extended to describe a stochastic process by spectral methods.

In order to demonstrate an application of the relatively simple spectral analysis for estimating the RST in an estuary from the migration of sand waves, sand wave measurements in the South Slough estuary, Coos Bay, Oregon were analyzed. This estuary is located on the southern Oregon coast approx 341 km south of the Columbia river entrance and 702 km north of the San Francisco Bay (see Fig. 1).

Background

The evolution of the various complex analytical models which describe the response of a deformable benthic interface to hydrodynamic forces is eloquently chronicled by Graf (7), Raudkivi (17), and Kennedy (9,10). This evolution follows essentially the same three conceptual areas described by Kinsman (11) for random surface gravity waves, i.e., hydrodynamics, stochastic processes and probability, and Fourier analysis. The evolution of the hydrodynamic concept began with Exner (compare to Ref. 7 or Ref. 17) who assumed that the bottom was initially a sinusoid and that the free surface of the water was sensibly horizontal. Exner's model is capable (at least theoretically) of including the effects of friction in a channel of variable width. The principal contribution of this model is that the instantaneous profile of the bed form results in a faster speed for the crest of the sinusoid compared to the trough and provides a means for estimating an approximate time for this sinusoid to become unstable and to collapse. Experimental verification of this model is lacking, as well as a physical explanation of how the bed initially becomes a sinusoid or what shape it assumes following the instability of breaking.

Others (6,12,15,18,19,21) have extended this model to include a steady flow over a sinusoidal bottom with a corresponding sinusoidal free surface. The linearized potential theory solution derived by these authors yields a disturbing singularity for the special case in which the speed of the free surface sinusoidal profile is exactly equal to the free stream velocity. The existence of this singularity is frequently used to argue that a deformable bedform may not remain flat. Kennedy (9,10) and Reynolds (18) also have included a slowly moving sinusoidal bottom in their model. However, the speed of this motion is considered to be small compared with the speed of the free-stream velocity and is neglected in the mathematical solution.

Mei (14) analyzed steady flow with a periodic free surface over an impermeable stationary bottom which also has a periodic profile. By considering the fully nonlinear boundary conditions and by assuming that the amplitude of the periodic bottom profile was of higher order in the perturbation parameter, he successfully removed the singularity present in the previous linearized studies and was able to determine the conditions required for the existence of a flat bottom. The key to his successful development was to assume that the bottom amplitude was of higher order in the perturbation parameter and that the speed of the free surface wave and the speed of the free-stream flow were *initially* equal.

The major limitations of each of these models for measuring the RST in an estuary with oscillatory flow is that only steady unidirectional flows are

treated and that the benthic boundaries are either impermeable or their motion must be determined empirically. The solution for the motion of an irregular, erodible, and permeable bottom under oscillatory flows does not presently exist.

Lee (13) developed a *stochastic* theory and analyzed the particle movement within a sand dune bed under uni-directional hydrodynamic flows. Lee (13) assumed that the process of alternate erosion and deposition of sand grains is stochastic and that the rest periods and step lengths of the sand particles within the profile are Gamma distributed. The Gamma distribution for the rest periods and the step lengths is a two-parameter positive semidefinite distribution. Once the Gamma distributions are determined for measured sand wave data collected in an estuary, the mode of the distributions of the rest periods, T_m, and the step lengths L_m could be used to estimate the RST in the estuary. The celerity of the sand wave would then be estimated by the relation $C = L_m/T_m$.

Hino (8) developed a *spectral* theory for sand waves also under uni-directional flows. He derived parametric equations for the wave number and frequency domain spectra for sand waves based on a dimensional analysis. The wave number and the wave frequency are related by the celerity for any harmonic of the sand wave profile in an estuary, which is given by

$$C = \frac{f}{k} \quad \text{(1)}$$

in which f = a harmonic frequency in the wave frequency spectrum; and k = a harmonic wave number in the wave number spectrum of the sand waves. The value of the peak frequency of the sand wave sprectrum, f_m, could provide an average estimate of the RST for the sand waves and could be estimated by Eq. 1 from the peak wave number and the celerity. The advantage of the *spectral* method of Hino (8) over the *stochastic* method of Lee (13) is that it would only be necessary to measure a spatial record of the sand wave elevations since the peak frequency of the frequency domain spectrum may be computed from Eq. 1 using a "dispersion" transformation between wave frequencies and wave numbers. In contrast, the *stochastic* method of Lee (13) requires both a temporal and a spatial record of the sand wave profile since no dispersion transformation presently exists between the Gamma distribution for step lengths and rest periods. A great deal of difficulty and expense is involved in obtaining a time-dependent record of a sand wave profile under field conditions since the profile sensor must be introduced into the flow field without significantly disturbing the flow. Furthermore, if the oscillatory motion of the wave-like benthic interface is a slowly-varying function of time, then the profile sensor must either be protected against long-term mechanical and biological degradation or repositioned exactly at the same location at relatively short intervals of time over a number of oscillatory cycles. This second requirement for repositioning may involve expensive navigational positioning systems.

Because of the potential economic savings offered by the *spectral* method of Hino (8) over the *stochastic* method of Lee (13) as a result of eliminating the requirement to measure a temporal record of the sand wave profile, the spectral method was adopted for application to the Bella-Williamson dissection plane approach. The essential theoretical elements from the eloquent derivation

of the Hino spectral method (8) are succinctly summarized for convenience in demonstrating its application.

Spectral Analyses of Sand Waves

The random, irregular shape of estuarine sand wave profiles may be represented by the harmonic analysis of a number of sinusoids of varying frequencies having spectral representation (compare Refs. 4, 5, and 22). Hino (8) derived the parametric equation for a wave number and a wave frequency spectrum for wave numbers; and frequencies within the equilibrium subrange for sand wave values are shown in Fig. 2.

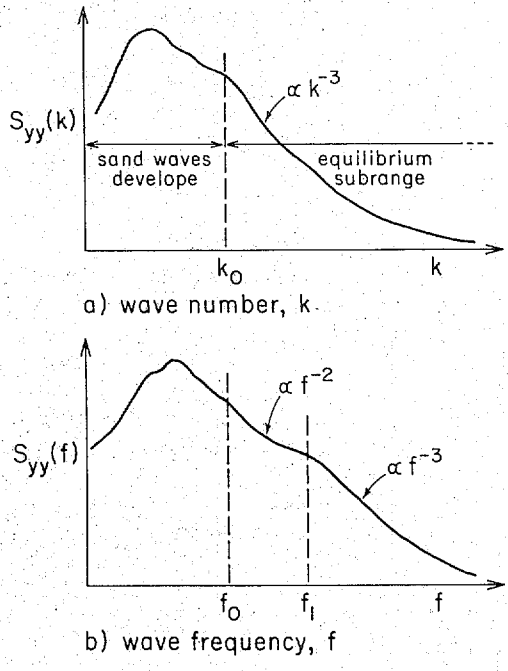

FIG. 2.—Equilibrium Sand Wave Spectra: (*a*) Wave Number Spectrum $S_{yy}(k)$; and (*b*) Wave Frequency Spectrum, $S_{yy}(f)$

For fully-developed (or equilibrium) sand waves, the slope of the sand bed profile may never exceed the angle of repose, ϕ, of the sand. This implies that an upper limit exists for the spectral amplitude values within an equilibrium subrange in which the spectral form is governed predominantly by the angle of repose and some power of the wave number. For lower values of wave numbers below this equilibrium subrange, the sand waves are still growing and the law of equilibrium subrange fails due to an instability mechanism between the sand bed and the flowing water as a result of the continuing transfer of energy from the hydrodynamic shear stress to the deformable sand bed.

Wave Number Spectrum.—The wave *number* spectrum may be estimated from a *spatial* record of a sand wave profile. From a dimensional analysis, Hino (see Ref. 8, Eq. 10) has determined that the spectral density function for a

sand wave profile within the equilibrium subrange is of the form

$$S_{yy}(k) = \alpha(\phi)\, k^{-3}; \quad (k_o << k << d^{-1}) \quad \ldots\ldots\ldots\ldots\ldots\ldots\ldots\ldots\ldots\ldots (2)$$

in which k = the wave number in cycles per unit length; $\alpha(\phi)$ = a function of the angle of repose of a sand particle (assumed to be a constant); d = the diameter of the sand particle; y = the vertical elevation of the sand wave profile above the horizontal mean at any horizontal coordinate in a spatial sand wave record (see Fig. 3); and k_o = the smallest value for the wave number of the sand wave field in which the interactional instability mechanisms are not important. Analyzing experimental data for uni-directional flow, Hino (8) found that an approximate value for k_o may be estimated from

$$k_o = \frac{0.15}{h} \quad \ldots\ldots\ldots\ldots\ldots\ldots\ldots\ldots\ldots\ldots\ldots\ldots\ldots\ldots\ldots\ldots\ldots\ldots (3)$$

in which h = the depth of water in the laboratory channel.

Wave Frequency Spectrum.—The wave frequency spectrum may be estimated from a *temporal* record of a sand wave profile. In contrast to the single "−3 power law" (see Eq. 2) throughout the wave *number* equilibrium subrange, Hino (8) suggests that there are two power laws for the wave *frequency* equilibrium subrange. This dual parametric law for the wave frequency equilibrium subrange

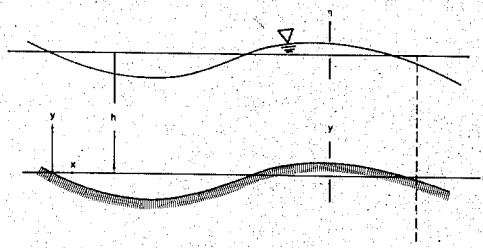

FIG. 3.—Definition Sketch for Sinusoidal Sand Bed

may be due, in part, to the form of the frequency dispersion transformation assumed by Hino (8). An alternate frequency dispersion transformation which removes this dual parametric law for the wave frequency equilibrium subrange is given in Appendix I.

Hino (8) assumes that within the equilibrium subrange, the frequency spectrum follows a "−3 power law" for higher frequencies, and a "−2 power law" for frequencies slightly greater than the spectral peak frequency but less than the "−3 power law" frequencies. In the higher frequency region within the equilibrium subrange, the frequency spectrum for the sand wave profile is assumed from dimensional analysis to be given by

$$S_{yy}(f) = f(\psi)\, V_*^2\, f^{-3}; \quad (f_1 < f < f_\infty) \quad \ldots\ldots\ldots\ldots\ldots\ldots\ldots\ldots\ldots\ldots (4)$$

in which f = the wave frequency in cycles per unit time; $f(\psi)$ = a function of ψ, which is a nondimensional quantity related to the critical tractive force of the sand bed by $\psi = V_*^2/[(\rho_s/\rho - 1)\, gd]$; V_* = the bed shear velocity; and f_1 and f_∞ = the lower and upper bounds, respectively, of the higher frequency

region within the equilibrium subrange for sand wave frequencies.

The wave number, k, and the wave frequency, f, of a sand wave are related by the wave celerity or rate of translation of the waveform according to

$$f = C(k)\,k \quad \ldots \quad (5)$$

The relationship between the frequency spectrum and the wave number spectrum may be determined by equating the areas under two differential intervals, Δk and Δf of the wave number and wave frequency spectral densities, respectively. Equating these differential areas yields

$$S_{yy}(f) = S_{yy}(k)\frac{dk}{df} \quad \ldots \quad (6)$$

which may be used to estimate the wave frequency spectrum without having to measure a temporal sand wave profile. In the lower wave number range for small values of the wave numbers below both the spectral peak wave number and the equilibrium subrange, energy transfer between the sand waves and the water flowing over them become predominant since the sand waves are still growing. Within this lower wave number range, the celerity must be considered to be a function of the wave number; i.e.

$$C(k) \propto k \coth 2\pi kh \quad \ldots \quad (7)$$

Within the equilibrium subrange for wave number values $k << 1/2\pi h$, Eq. 7 may be approximated by

$$C(k) = \gamma k \quad \ldots \quad (8)$$

in which γ = a dimensional constant with dimensions L^2/T. Substituting Eq. 8 into Eq. 5, and taking derivatives on both sides, we obtain

$$\frac{dk}{df} = \frac{1}{2\gamma k} \quad \ldots \quad (9)$$

The equilibrium subrange of the wave number spectrum must extend to wave numbers which are lower than for the equilibrium subrange of the frequency spectrum (8). The equation for the frequency spectral density function for this relatively lower frequency region below the wave frequency equilibrium subrange may now be obtained by substituting Eqs. 2 and 9 into Eq. 6; i.e.

$$S_{yy}(f) = \frac{1}{2}\alpha(\phi)\,\gamma f^{-2}; \quad (f_o) < f < f_1) \quad \ldots \quad (10)$$

in which f_o = the lowest value for the wave frequency in the wave spectrum and corresponds to the lowest wave number, k_o.

In summary, within the equilibrium subrange for the wave number spectrum, Hino (8) concludes that there must be two different frequency regions for the corresponding wave frequency spectrum. He gives the following two forms for the wave frequency spectrum within this corresponding wave number equilibrium subrange: (1) The "-2 power law" of Eq. 10: $S_{yy}(f) = (1/2)\,\alpha(\phi)\,\gamma f^{-2}$, $(f_o < f < f_1)$; and (2) the "-3 power law" of Eq. 4: $S_{yy}(f) = f(\psi)\,V_*^2 f^{-3}$, $(f_1 < f < f_\infty)$. The key to the successful application of the spectral

method for estimating the RST lies in determining the appropriate constant of proportionality, γ, and the angle of repose function, $\alpha(\phi)$.

For application in the Bella-Williamson RST-OCS dissection plane method, it was proposed to use the total energy content of the sand wave number spectral density (or, equivalently, the variance of the spatial profile record) and the wave number equilibrium subrange defined by Hino (8) as measures of the RST in an estuary in which sand waves are present. The relative magnitude of the total energy in the sand wave profile and the equilibrium subrange amplitudes would provide estimates of the relative energy transfer occurring between the hydrodynamic shear stress and the resulting deformation of the migrating benthic interface. For comparison, data were measured in both a *pristine* estuary and an adjacent *developed* (dredged) estuary. The relative ease and low cost involved in acquiring these sand wave records are especially attractive economically and are fundamentally compatible with the philosophy of the Bella-Williamson RST-OCS dissection plane approach in the evaluation and preparation of EIS for dredging operations in estuaries.

Sand Wave Data Acquisition and Analysis

Sand wave profiles were recorded in analog form by a submerged sonic profiler during a two-day period. A rigid steel pipe was mounted vertically to the side of a boat and the sonic transducer was secured to the underwater end approx 0.8 m above the sand bed. The sonic data were recorded directly on FM magnetic tape in analog form by an FM tape recorder aboard the boat. The sonic sampling locations (STA 1, 2, 3) are shown in Fig. 1.

Five buoys were implanted along the channel at each of the sampling stations shown in Fig. 1 and the distances between these buoys were measured by means of a range finder (transit type) on shore. The buoys were moored taut and anchored to the bottom of the estuary in order to minimize their drift. Before recording the sonic data at each station, the boat was driven slowly along the course of the buoys and the time of travel between the buoys was recorded by a stop watch. The speed of the boat was then computed by dividing the known distances between the buoys by the recorded time required for the boat to cover these distances at each station. The speed of the boat was approximately equal to 0.5 m/sec. The speed of the boat at each station was then maintained at approximately a constant value of 0.5 m/sec during each of the subsequent data recording operations. During the two-day data-recording period, two data recordings were taken at STA 1, four at STA 2, and one at STA 3. These seven data measurements are summarized in Table 1.

In order to correlate the *in situ* length of the sand waves with the magnetic tape data, the passing of each buoy by the sampling boat was recorded by voice on the same channel of the magnetic tape as the sonic data. The pulse rate for the sound waves from the sonic profiler was 1/30 second. This rate of data sampling was required to be greater than the speed at which the boat was moving (approx 0.5 m/sec) in order to insure that no sand wave elevation data were omitted from the recordings. In order to eliminate extraneous vertical disturbances to the boat and, consequently, to the data records, data were collected only when the water surface disturbances were minimum. In order to maintain a sufficient draft below the underwater sonic transducer, data were

collected only during the slack periods of high tide.

These sonic sand wave data were recorded in analog form on an FM magnetic tape and were later copied onto an analog strip chart for visual observation and calibration. The total length of each run was computed both in meters and in seconds. The elapsed time between the start and the end of each FM magnetic tape record gave the total length of the record in seconds. The total length of the sand wave records in seconds was required in order to digitize the sand wave record by an analog to digital converter (ADC) through a PDP 11 E10 minicomputer. The spatial resolution, Δx, of each sand wave record was computed by multiplying the tangent of the sonic profiler half-beam angle (5°) by the vertical height of the sonic transducer above the sand bed (approx 0.8 m). The spatial resolution, Δx, computed from the aforementioned method was approximately equal to 0.07 m. This spatial resolution was then compared with the horizontal distance between two consecutive sonic waves to insure that it was greater than the horizontal distance between two consecutive sonic waves.

TABLE 1.—Summary of Sonic Profiler Data

Record number (1)	Length, in meters (2)	Length, in seconds (3)	Variance, in square meters (4)	H_{rms}, in meters (5)	Δk, in meters (6)	k_o, in meters (7)	Sampling location, (see Fig. 1) (8)
1	91.09	236	0.0113	0.30	0.011	0.075	STA 1
2	127.53	471	0.1348	1.04	0.008	0.075	STA 1
3	211.34	675	0.0615	0.70	0.005	0.038	STA 2
4	211.34	400	0.0337	0.52	0.005	0.038	STA 2
5	211.34	402	0.0654	0.72	0.005	0.038	STA 2
6	216.02	540	0.0427	0.58	0.005	0.038	STA 2
7	45.81	270	0.2382	1.38	0.022	0.017	STA 3

This horizontal distance was computed by multiplying the average speed of the boat by the rate at which the sonic waves were sent. Once the spatial resolution of each record was determined, the total number of digitizing values, N, may be computed from the relation

$$N \geq \frac{L}{\Delta x} \qquad (11)$$

in which N = the total number of digitizing values; and L = the total length of the sand wave profile in meters. The digitizing rate required for the ADC, Δt, was then computed from the relation

$$\Delta t = \frac{T}{N} \qquad (12)$$

in which T = the total time of the record in seconds obtained from the analog magnetic tape.

The digital spatial sand wave data were first linearly detrended by a numerical algorithm and then the amplitude spectra were estimated by an integer finite

Fourier transform (FFT) algorithm of base two. For a real-valued sequence, y_n, the discrete FFT pair may be given by

$$y_n = N^{-1} \sum_{m=o}^{N-1} A_m \exp i\left(\frac{2\pi nm}{N}\right); \quad n = 0, 1, 2, \ldots, N-1 \quad \ldots\ldots\ldots (13a)$$

$$A_m = \sum_{n=o}^{N-1} y_n \exp -i\left(\frac{2\pi nm}{N}\right); \quad m = 0, 1, 2, \ldots, N-1 \quad \ldots\ldots\ldots (13b)$$

in which the real and imaginary components of the complex-valued FFT coefficients are identified by

$$A_m = RA_m + iIA_m \quad \ldots\ldots\ldots (14)$$

In order for the inverse transform to be exact, we must also require that

$$\Delta t \cdot \Delta k = N^{-1} \quad \ldots\ldots\ldots (15)$$

Only the real part of the complex-valued (y_n) sequence represents the digitized values of the sand wave profiles. The one-sided spectral density function for the sand wave profile may be estimated from the complex-valued FFT coefficients according to

$$S_{yy}(m\Delta k) = \frac{2A_m \cdot A_m^*}{\Delta k}; \quad m = 0, 1, 2, \ldots, \frac{N}{2} \quad \ldots\ldots\ldots (16)$$

in which the superscript asterisk denotes a complex conjugate value. The amplitude spectra for the sand waves recorded at the three stations in Coos Bay estuary are shown in Figs. 4–9. The variance, root-mean-square wave height, H_{rms}, and the equal discrete wave number interval, Δk, are tabulated in Table 1. The variance of the zero-mean spatial sand wave profile is computed from

$$V = \frac{1}{N} \sum_{n=o}^{N-1} y_n^2 \quad \ldots\ldots\ldots (17)$$

and the H_{rms} from

$$H_{\text{rms}} = \left\{ 8\,\Delta k \sum_{m=o}^{N/2} S_{yy}(m\Delta k) \right\}^{1/2} \quad \ldots\ldots\ldots (18)$$

The amplitude spectra of the sand wave records from the South Slough estuary, Coos Bay, Oregon (see Figs. 4–8) demonstrate two important points. First, the total energy (or, equivalently, the statistical variance of the spatial sequence) of the spectra are relatively low (e.g., the minimum $H_{\text{rms}} = 0.3$ m for record No. 1 in Fig. 4). Second, most of the energy is contained in the fundamental harmonic component. This indicates that the dynamic migration of these sand waves is a slowly-varying, low-energy process and that the sand bed is a slowly-undulating boundary. In addition, the maximum spectral amplitudes are found at wave numbers which lie below the smallest wave number of the equilibrium subrange given by Hino (8) for uni-directional flow in the laboratory. This indicates that the sand waves in the South Slough estuary are still growing. In estuaries of low sand wave energy, catastrophic events such as storms govern the RST and not the hydrodynamics of the average flow. In the South Slough

estuary data, the rms sand wave height, H_{rms}, varied from 0.30 m–1.04 m.

In contrast, sand waves in the Coos Bay main channel (see Fig. 9) have a higher energy content (variance of the spatial sequence) dispersed over a wider band of wave numbers; however the fundamental harmonic still contains most of the total energy. This is due to the stronger tidal velocities probably

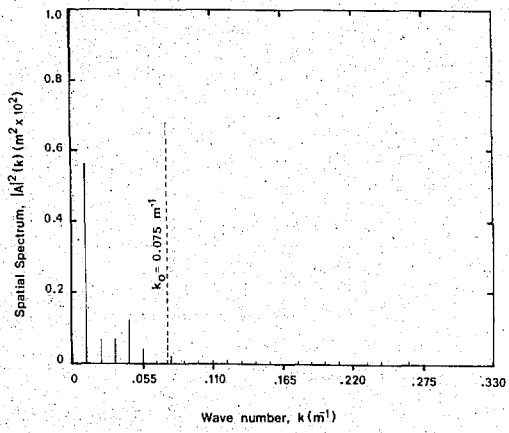

FIG. 4.—Sand Wave Amplitude Spectrum for Record No. 1 ($V = 0.0113\ m^2$; $\Delta k = 0.011\ m^{-1}$)

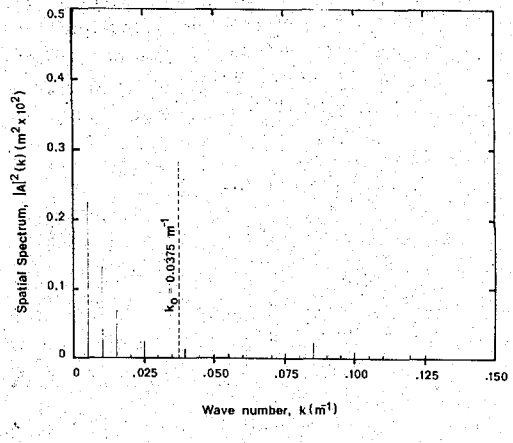

FIG. 5.—Sand Wave Amplitude Spectrum for Record No. 3 ($V = 0.0615\ m^2$; $\Delta k = 0.005\ m^{-1}$)

augmented by the ship propeller disturbances in the main channel. Since this spectral comparison is only a visual comparison, the spectral band width parameter which provides an estimate of the width of the wave frequency spectrum (compare to Ref. 3), should be computed from the wave frequency spectrum in order to obtain the dispersion of the spectrum about the spectral peak. The sand wave frequency spectrum may be obtained from the wave number spectrum

by using a theoretical or empirical transformation between the wave numbers and the wave frequencies. A flow chart for obtaining the RST from a wave number spectrum using a dispersion transformation is shown in Fig. 10.

For the sand wave record from the Coos Bay main channel (see record No. 7 in Fig. 9), the wave number of the maximum spectral amplitude falls very

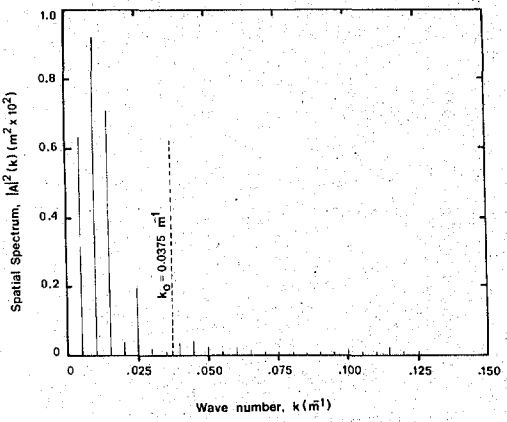

FIG. 6.—Sand Wave Amplitude Spectrum for Record No. 4 (V = 0.0337 m^2; Δk = 0.005 m^{-1})

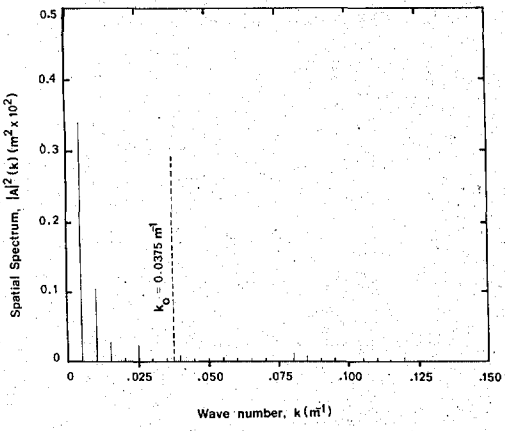

FIG. 7.—Sand Wave Amplitude Spectrum for Record No. 5 (V = 0.0654 m^2; Δk = 0.005 m^{-1})

close to the minimum wave number value for the equilibrium subrange given by Hino (8). We note that the minimum wave number value for the equilibrium subrange, k_o, given by Hino (8) is slightly less than the first harmonic component. This demonstrates that some additional care must be taken when digitizing analog data in order to insure that the value for the minimum wave number for the equilibrium subrange, k_o, will be much greater than the fundamental harmonic component.

For example, if we assume that k_o will appear in the mth harmonic (e.g., $k_o = m\,\Delta k$; $m >> 1$), then the equal discrete wave number interval, Δk, may be estimated from Eq. 3 according to

$$\Delta k = \frac{0.15}{m\,h} \quad \ldots\ldots\ldots\ldots\ldots\ldots\ldots\ldots\ldots\ldots\ldots\ldots\ldots\ldots\ldots\ldots\ldots\ldots\ldots\ldots\ldots\ldots \quad (19)$$

From this value of Δk and the spatial resolution, Δx, computed from an analysis

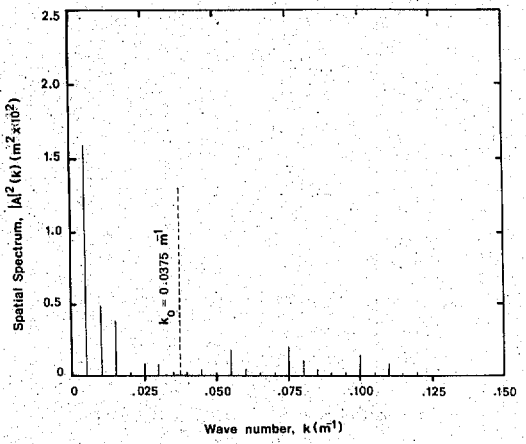

FIG. 8.—Sand Wave Amplitude Spectrum for Record No. 6 (V = 0.0427 m^2; Δk = 0.005 m^{-1})

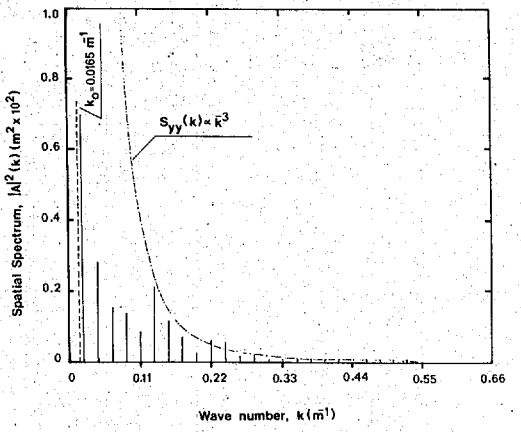

FIG. 9.—Sand Wave Amplitude Spectrum for Record No. 7 (V = 0.2382 m^2; Δk = 0.022 m^{-1})

of the data acquisition system, the total number of digitized values, N, may be computed from:

$$N = (\Delta x \cdot \Delta k)^{-1} \quad \ldots\ldots\ldots\ldots\ldots\ldots\ldots\ldots\ldots\ldots\ldots\ldots\ldots\ldots\ldots\ldots\ldots\ldots\ldots\ldots\ldots\ldots \quad (20)$$

For the Coos Bay main channel, if we assume that k_o will appear in the fifth

harmonic, then the equal discrete wave number interval, Δk, may be estimated from Eq. 19 to be $\Delta k = 0.0033\ m^{-1}$. Substituting this equal discrete wave number interval into Eq. 20 yields approx $N \simeq 4{,}096$. Therefore, the spatial sand wave data should have been digitized with at least 4,096 values instead of the 1,024 values used in the present analysis, in order to insure that k_o would be much greater than the fundamental harmonic component and to better resolve the equilibrium subrange.

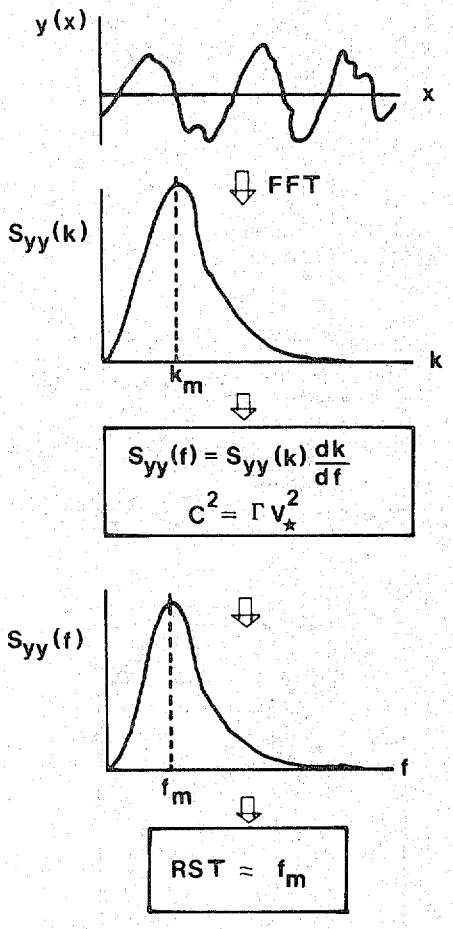

FIG. 10.—Flow Chart for Estimating RST from Wave Number Spectrum by Dispersion Transformation

These amplitude spectra demonstrate the significant differences between the hydrodynamic processes in a *pristine* estuary (South Slough) and a *developed* estuary (Coos Bay Main Channel). The RST in the pristine estuary is a low-energy process, which is storm driven, while the RST in the developed estuary is a high-energy process driven by the hydrodynamics of the average flows. Additional laboratory and field measurements are required, however, to verify

the constants of proportionality for the equilibrium subrange and the dispersion transformation.

Conclusions

The equilibrium subrange and the total energy (variance of the spatial sequence) of the wave number spectrum for sand waves in an estuary may be used to quickly and economically locate the RST in the Bella-Williamson dissection plane method for diagnosing the chronic environmental impacts of dredging in estuaries. A spatial record of a sand wave profile in an estuary may be easily measured by underwater sonic profilers and the wave number spectral amplitude may be quickly estimated by an FFT algorithm. A comparison between the rms wave height (which may be determined from the total energy content computed by the FFT coefficients) with the equilibrium subrange of the theoretical wave number spectrum developed by Hino (8) provides a reasonable estimate for a measure of the RST. Some care must be taken in both recording and digitizing spatial sand wave data and the important analytical relationships between the spatial resolution of the data acquisition equipment, the speed of the sampling boat, and the minimum value of the equilibrium subrange wave number are presented.

The method described in the present analysis may be extended to compute the wave frequency spectrum *without* requiring the measurement of a temporal sand wave profile provided that a dispersion transformation between wave frequencies and wave numbers is known. A uniform "−3 power law" wave frequency spectrum is presented which follows the assumption that the wave celerity is proportional to the bed shear velocity. Additional analytical, or experimental verifications, or both, are required to determine the dimensionless constant of proportionality for oscillatory flows.

The potential economic savings which may be realized in the preparation and evaluation of EIS by the judicious application of the Bella-Williamson dissection approach are tremendously encouraging. A key ingredient in their approach is the successful integration of disciplinary data and analysis which may be rapidly and economically collected and analyzed. The spectral analysis of sand wave profiles by an FFT in an estuary is presented within the context of a disciplinary input to the Bella-Williamson dissection plane method. Details regarding the integration of disciplinary data are given by Bella and Williamson (2). In addition, recommendations are presented for extending the present knowledge of the wave number equilibrium subrange and the wave frequency dispersion transformation for sand waves under oscillatory flows.

Acknowledgments

We are especially grateful for the unique opportunity to provide disciplinary data to D. A. Bella and K. J. Williamson for integration in the development of their pioneering work on the RST-OCS dissection plane approach for diagnosing the chronic impacts of dredging in estuaries which was sponsored by the National Science Foundation-Research Applied to National Needs (NSF-RANN) under Grant No. ENV71-01908. Equally rewarding and professionally stimulating have been the collaborative opportunities with the following NSF-RANN team

members: W. L. Schroeder, L. S. Slotta, D. R. Hancock, C. K. Sollitt, and J. M. Stander. The sonic profiler used in the data acquisition was made available by C. Nordin of the United States Geological Survey, Department of the Interior. Additional financial support (for RTH) was provided by the Oregon State University Sea Grant College Program, National Oceanic and Atmospheric Administration, Office of Sea Grant, Department of Commerce, under Grant No. 04-6-158-44004. We dedicate this effort to the memory of our late NSF-RANN team member J. E. McCauley, benthic biologist, educator, and a good man. It is also a pleasure to extend our appreciation to the reviewers for their valuable suggestions on how to improve both the clarity and accuracy of our efforts.

Appendix I.—Uniform "−3 Power Law" Equilibrium Frequency Spectrum

The equilibrium wave frequency spectra derived by Hino (8) follows a "−3 power law" for the higher frequencies within the equilibrium subrange and a "−2 power law" for frequencies slightly greater than the spectral peak frequency but less than the "−3 power law" frequencies. This indicates that two frequency dispersion relationships are required for the sand waves *within* the wave number equilibrium subrange. Since the wave frequency spectrum is of prime importance in the estimation of the RST, a uniform "−3 power law" is developed for the entire wave frequency equilibrium subrange. This results in a one-to-one correspondence with the wave number equilibrium subrange.

Following the derivation for the equilibrium subrange for surface gravity waves by Phillips (16), we note two important points. First, the constants of proportionality used in his dimensional analysis are dimensionless; and, second, the same dimensional constant used in the parametric equation for the wave frequency spectrum also appears in the frequency dispersion equation (i.e., the gravitational constant). We shall incorporate these two points in our following formulation.

Gradowczyk (6) and Hino (see Ref. 8, Eq. 16) have shown that the celerity of the sand wave profile is proportional to the bed shear velocity. We, therefore, assume the following for the frequency dispersion transformation given by Eq. 8:

$$C^2 = \Gamma V_*^2 \qquad (21)$$

in which Γ = a *dimensionless* constant of proportionality. Eq. 9 now becomes

$$\frac{dk}{df} = \frac{1}{\Gamma^{1/2} V_*} \qquad (22)$$

Substituting this differential relationship into Eq. 6 yields

$$S_{yy}(f) = \alpha(\phi)(\Gamma V_*)^2 f^{-3}; \quad (f_o < f < f_\infty) \qquad (23)$$

The lowest frequency, f_o, now corresponds to the lowest wave number, k_o, in the equilibrium subrange given by Hino (8).

The upper wave number range in the equilibrium subrange is assumed by Hino (8) to be given by

$$k << d^{-1} \qquad (24)$$

in which d = the diameter of the sand particle. Accordingly, the upper frequency limit, f_∞, may be found to be

$$f_\infty << \Gamma^{1/2} V_* d^{-1} \quad \ldots \quad (25)$$

and a uniform "−3 power law" for the entire wave frequency equilibrium subrange is now given by

$$S_{yy}(f) = \alpha(\phi)(\Gamma V_*)^2 f^{-3}; \quad (f_o < f < \Gamma^{1/2} V_* d^{-1}) \quad \ldots \quad (26)$$

Appendix II.—References

1. Bella, D. A., and Overton, W. S., "Environmental Planning and Ecological Possibilities," *Journal of the Sanitary Engineering Division*, ASCE, Vol. 98, No. SA3, Proc. Paper 8994, June, 1972, pp. 579–592.
2. Bella, D. A., and Williamson, K. J., "Diagnosis of Chronic Impacts of Estuarine Dredging," *Journal of Environmental Systems*, Vol. 9, 1979–1980, pp. 289–311.
3. Cartwright, D. E., and Longuet-Higgins, M. S., "The Statistical Distribution of the Maxima of a Random Function," *Proceedings Royal Society of London*, Series A, Vol. 237, 1956, pp. 212–232.
4. Cartwright, D. E., "On Submarine Sand-Waves and Tidal Lee-Waves," *Proceedings of Royal Society of London*, Series A, Vol. 253, 1959, pp. 218–240.
5. Crickmore, M. J., and Lean, G. H., "The Measurement of Sand Transport by Means of Radioactive Tracers," *Proceedings of Royal Society of London*, Series A, Vol. 266, 1962, pp. 402–421.
6. Gradowczyk, M. H., "Wave Propagation and Boundary Instability in Erodible-bed Channels," *Journal of Fluid Mechanics*, London, England, Vol. 33, 1968, pp. 93–112.
7. Graf, W. H., *Hydraulics of Sediment Transport*, McGraw-Hill Book Co., Inc., New York, N.Y., 1971, pp. 273–303.
8. Hino, M., "Equilibrium-Range Spectra of Sand Waves Formed by Flowing Water," *Journal of Fluid Mechanics*, London, England, Vol. 34, 1968, pp. 565–573.
9. Kennedy, J. F., "The Mechanics of Dunes and Antidunes in Erodible-Bed Channels," *Journal of Fluid Mechanics*, London, England, Vol. 16, 1963, pp. 521–544.
10. Kennedy, J. F., "The Formation of Sediment Ripples, Dunes and Anti-Dunes," *Annual Review of Fluid Mechanics*, Annual Reviews, Inc., Palo Alto, Calif., 1969, pp. 147–168.
11. Kinsman, B., *Wind Waves*, Prentice-Hall, Inc., Englewood Cliffs, N.J., 1956, pp. 51–112, 325–361, 427–487.
12. Lamb, H., *Hydrodynamics*, 6th ed., Dover Publications, Inc., New York, N.Y., 1945, pp. 398–410.
13. Lee, B. K., "Stochastic Analysis of Particle Movement Over a Dune Bed," thesis presented to Colorado State University, at Fort Collins, Colo., in 1973, in partial fulfillment of the requirements for the degree of Doctor of Philosophy.
14. Mei, C. C., "Steady Free Surface Flow Over Wavy Bed," *Journal of the Engineering Mechanics Division*, ASCE, Vol. 95, No. EM6, Proc. Paper 6967, Dec., 1969, pp. 1393–1402.
15. Milne-Thompson, L. M., *Theoretical Hydrodynamics*, 5th ed., The MacMillan Co., New York, N.Y., 1969, p. 444.
16. Phillips, O. M., *Dynamics of the Upper Ocean*, Cambridge University Press, Cambridge, England, 1966, pp. 109–119.
17. Raudkivi, A. J., *Loose Boundary Hydraulics*, Pergamon Press, Inc., New York, N.Y., 1967, pp. 175–221.
18. Reynolds, A. J., "Waves on an Erodible Bed of an Open Channel," *Journal of Fluid Mechanics*, London, England, Vol. 22, 1965, pp. 113–133.
19. Shinbrot, M., "Water Waves Over Periodic Bottom in Three Dimensions," *Journal Institute Mathematics and Applications*, Vol. 25, 1980, pp. 367–385.
20. *The National Environmental Policy Act*, (PL 91-190), 42 U.S.C. 4321 *et seq*, 1969, Sec. 101(b) and 102(2)(C).
21. Wehausen, J. V., "Surface Waves," *Handbuch der Physik*, Vol. 9, Julius Springer, Berlin, Germany, 1960, pp. 569–570.
22. Winant, C. D., Inman, D. L., and Nordstrom, C. E., "Description of Seasonal Beach Changes Using Empirical Eigenfunctions," *Journal of Geophysical Research*, Vol. 80, No. 15, 1975, pp. 1979–1986.

APPENDIX III.—NOTATION

The following symbols are used in this paper:

$A(\cdot)$ = complex finite Fourier transform (FFT) coefficient;
C = celerity of sand wave;
d = diameter of sand particle;
f = sand wave frequency;
f_1, f_∞ = lower and upper frequency bounds for the "−3 power law" equilibrium subrange (8);
f_o = lowest frequency in the equilibrium subrange;
f_m = peak frequency of the wave frequency spectrum;
$f(\psi)$ = a function of ψ;
H_{rms} = root mean square wave height;
h = depth of water in channel;
I = imaginary part of complex FFT coefficient;
$i = \sqrt{-1}$ = imaginary unit number;
k = wave number (cycles/length);
k_o = smallest wave number in the equilibrium subrange;
k_m = peak wave number of the wave number spectrum;
L = length of sand wave record;
L = wave length of a sand wave;
N = total number of digitizing values;
R = real part of a complex FFT coefficient;
$S_{yy}(\cdot)$ = spectral density function for the sand wave profile;
T = total time of the sand wave record;
T = wave period of a sand wave;
V = variance of the sand wave spatial profile;
V_* = shear velocity;
x = horizontal coordinate axis;
y = instantaneous vertical elevation of sand wave profile measured positive upwards from horizontal bottom;
$\alpha(\phi)$ = function of ϕ;
Γ = dimensionless constant of proportionality for frequency dispersion;
γ = dimensional constant of proportionality for frequency dispersion (8);
Δk = equal discrete wave number interval;
Δt = equal discrete time interval;
Δx = equal discrete spatial interval;
ρ = fluid density;
ρ_s = density of sand particles;
ϕ = angle of repose of a sand particle; and
ψ = nondimensional quantity related to the critical tractive force of the sand bed.

16016 EVALUATION OF SAND WAVES IN AN ESTUARY

KEY WORDS: Dissection; **Ecosystems;** Energy; Environmental impact statements; Equilibrium; **Estuaries; Sand waves; Sediment; Spectral analysis;** Turnovers

ABSTRACT: The Bella-Williamson rate of sediment turnover-organic content of sediment (RST-OCS) dissection plane method integrates relevant physical, chemical, and biological analyses in order to estimate the chronic impacts of dredging on estuarine ecosystems. A spectral analysis by a finite Fourier transform of estuarine sand waves is presented which only requires a spatial sand wave record that is relatively easy to measure in contrast to stochastic analyses which require both spatial and temporal observations of sand wave profiles. The total energy content (or, equivalently, the statistical variance of the spatial sand wave profile) and the equilibrium subrange of the wave number spectrum provide readily observable measures of the RST in an estuary; economic savings, promise to be significant. In addition, a uniform "-3 power law" for the wave number equilibrium subrange is presented which offers an opportunity to obtain a sand wave frequency spectrum without a temporal sand wave profile record through a dispersion transformation proportional to the bed shear velocity.

REFERENCE: Baliga, B. R., and Hudspeth, Robert T., "Evaluation of Sand Waves in an Estuary," *Journal of the Hydraulics Division,* ASCE, Vol. 107, No. HY2, **Proc. Paper 16016,** February, 1981, pp. 161-178

The Oregon State University Sea Grant College Program is supported cooperatively by the National Oceanic and Atmospheric Administration, U.S. Department of Commerce, by the State of Oregon, and by
private industry.